Observational Study

Medicine®

OPEN

Dynamic enhancement patterns of small-diameter mass-forming intrahepatic cholangiocarcinomas on contrast-enhanced magnetic resonance imaging

Challenges faced by the radiologist

Wenjie Liang, MD[a,b], Dalong Wan, MD[b], Qinyan Lu, MD[c], Shengzhang Lin, MD[b], Zhihua Chen, MD[d,*]

Abstract

Contrast-enhanced magnetic resonance imaging (MRI) characteristics of small-diameter mass-forming intrahepatic cholangiocarcinomas (ICCs) (diameter ≤3 cm) are still unclear.

This study focused on imaging findings of small mass-forming ICCs. The MRI findings for small-diameter mass-forming ICCs were summarized, and the enhancement features of small ICC nodules with different diameters [2 groups were defined: a smaller nodule group (ICC diameter <2 cm) and a larger nodule group (ICC diameter >2 cm)] were compared on contrast-enhanced MRI.

In our study, there were 41 small ICC nodules in 41 patients, including 30 men and 11 women (average age, 56 years). The nodules were characterized by peripheral hyperintense in the arterial phase on contrast-enhanced MRI. In the different diameter groups, peripheral hyperintense was the most common in the larger nodule group (56% vs 12%, $P < .05$) and hypointense was more common in the smaller nodule group (25% vs 0%, $P < .05$) in the arterial phase on contrast-enhanced MRI. Smaller nodules mainly showed progressive enhancement, whereas larger nodules mainly showed peripheral continuous enhancement (56% vs 6%, $P < .05$).

The small-diameter mass-forming ICC nodules mainly show peripheral continuous enhancement on contrast-enhanced MRI; however, those with diameters <2 cm commonly show progressive enhancement.

Abbreviations: AFP = α-fetoprotein, ALT = alanine aminotransferase, AST = aspartic transaminase, CA 125 = carbohydrate antigen 125, CA 199 = carbohydrate antigen 199, CEA = carcinoembryonic antigen, DBIL = direct bilirubin, dCCA = distal cholangiocarcinoma, HCC = hepatocellular carcinoma, IBIL = indirect bilirubin, ICC = intrahepatic cholangiocarcinoma, LI-RADS = Liver Imaging Reporting and Data System, MRI = magnetic resonance imaging, pCCA = perihilar cholangiocarcinoma, T1WI = T1-weighted imaging, T2WI = T2-weighted imaging, TBIL = total bilirubin.

Keywords: imaging, intrahepatic cholangiocarcinoma, magnetic resonance imaging

1. Introduction

Intrahepatic cholangiocarcinoma (ICC) localizes within the liver parenchyma and originates from the biliary tree epithelium below the secondary intrahepatic branches.[1] Extrahepatic cholangiocarcinoma is relative to the anatomical location, including perihilar and distal cholangiocarcinoma (dCCA), which are common types of cholangiocarcinoma and constitute the second most common type of liver tumor,[2] accounting for approximately 3% in all gastrointestinal tumors and approximately 10% to 25% of primary malignant liver tumors.[3,4] Although ICC accounts for slightly less than 10% of cholangiocarcinoma cases,[5] over the past few decades in the United States, the incidence of cholangiocarcinoma has increased by approximately 22%, primarily due to an increase in the detection rate of ICC.[6] Cholangiocarcinoma-associated mortality has also increased by 39% over the same time period.[6] Worldwide, there have been increases in ICC morbidity and mortality, including in almost all Western countries, although the distribution of the disease varies.[7] Approximately 60% to 70% of patients with ICC have nonresectable tumors,[7] which greatly influences the treatment strategies used with and the prognoses of these patients. Thus, early detection and diagnosis of ICC are essential.

Editor: Weisheng Zhang.

The study was supported by the Natural Science Foundation of Zhejiang Province, China (Grant No. LY17H160010), the Foundation of Health and Family Planning Commission of Zhejiang Province (Grant No. 2016KYB084), and the Foundation of the Key Project of Medicine (Grant No. G3221).

The authors report no conflicts of interest.

[a] Department of Radiology, [b] Department of Hepatobiliary and Pancreatic Surgery, The First Affiliated Hospital, College of Medicine, Zhejiang University, [c] Department of Radiology, Hangzhou Aeromedicine Evaluation and Training Center of the PLA Air Force, Hangzhou City, Zhejiang Province, [d] Department of General Surgery, The First people's Hospital of Taicang City, Taicang Affiliated Hospital of Soochow University, Suzhou City, Jiangsu Province, China.

[*] Correspondence: Zhihua Chen, Department of General Surgery, The First people's Hospital of Taicang City, Taicang Affiliated Hospital of Soochow University, 58 Changshengnan Road, Taicang City, Jiangsu Province, China 215400 (e-mail: cztchos@163.com).

Medicine (2017) 96:43(e8351)

Received: 17 May 2017 / Received in final form: 9 August 2017 / Accepted: 24 September 2017

http://dx.doi.org/10.1097/MD.0000000000008351

As medical imaging technology and diagnostics have improved, magnetic resonance imaging (MRI) methods have become widely used in clinical examinations. The 2014 version of the Liver Imaging Reporting and Data System (LI-RADS) was designed to standardize the radiologic diagnosis of hepatocellular carcinoma (HCC).[8] The major criteria for diagnosis include size, arterial enhancement, capsule, washout, and threshold growth. The imaging features of ICCs with non-HCC malignancy have also been described[8]; these include peripheral enhancement, peripheral continuous enhancement, liver surface retraction, and relevant intrahepatic biliary dilatation. Although it is known that typical ICC has a different appearance than HCC on contrast-enhanced MRI,[1,7,9] a certain percentage of ICCs exhibit atypical imaging features, especially those with diameters $\leq$30 mm.[10,11] Although some scholars have confirmed that ICCs with different diameters have different imaging features,[12–15] the MRI enhancement characteristics of small ICCs with varying diameters remain to be defined.

Therefore, the present study aimed to investigate the enhancement characteristics of small ICCs with varying diameters on contrast-enhanced MRI. The dividing interval in imaging classification of LI-RADS HCCs was 2 cm in diameter.[8] Therefore, the comparison of MRI manifestations in this study was made among groups divided by this interval.

2. Patients and methods

2.1. Patients and clinical data

This retrospective study was approved by the Ethics Committee of First Affiliated Hospital, College of Medicine, Zhejiang University. Informed written consent was obtained from all patients. All methods were performed in accordance with the relevant guidelines and regulations. We searched the pathology database records of the hospital from January 2009 to June 2016. Our search terms included "intrahepatic cholangiocarcinoma" and "cholangiocarcinoma." Cases meeting the following criteria were included: pathological diagnosis of cholangiocarcinoma, excluding hepatocellular cholangiocarcinoma, and metastatic cholangiocarcinoma; lesion that originated in the secondary bile duct and its branch, with a lesion diameter not more than 3 cm with or without lymphatic metastasis, excluding hilar cholangiocarcinoma and dCCA; pathologic morphology of mass-forming cholangiocarcinoma, excluding periductal-infiltrating, intraductal-growth and other subtypes; and complete clinical and imaging data, including unenhanced and contrast-enhanced MRI scans, available for retrospective evaluation. In total, 41 patients with small ICC were included in this study. We reviewed the patients' clinical data, imaging findings, and pathological data with a focus on the imaging findings.

The medical records of the patients in this study were exported from the hospital's medical record management system. We summarized the patients' main clinical symptoms, signs, medical histories, and select laboratory results. The included laboratory indices were detection of hepatitis virus, inspection of liver function, and evaluation of tumor markers. The patients' smoking and drinking habits were also recorded.

2.2. Magnetic resonance imaging scans

Liver MRI scans were performed with a 3.0 T MRI machine (Signa HDx, GE Medical Systems, Milwaukee, WI) with 8-channel abdominal phased array coils (8US TORSOPA, GE Medical Systems) and respiratory gating; the scan range was from the diaphragmatic dome to the inferior margin of the liver. The routine T2-weighted imaging (T2WI) sequence used an FSE-XL array with the following parameters: repetition time (TR) = 7059 ms, echo time (TE) = 86.5 ms, slice thickness = 6 mm, interlayer spacing = 2 cm, and number of excitations (NEX) = 2. The in-phase and out-of-phase T1-weighted imaging (T1WI) used the following GRE sequence: TR = 220 ms, TE = 1.2 ms, and slice thickness = 5 mm. The diffusion sequence used the spin-echo version of echo planar imaging (SE-EPI): TR = 5600 ms, TE = 66 ms, thickness = 5 mm, and b value = 0 and 1000 s/mm^2. Enhanced scans used dynamic contrast-enhanced [phase gradient echo liver-accelerated volume array) scans and the array spatial sensitivity encoding technique: TR = 2.8 ms, TE = 1.3 ms, scanning slice thickness = 5 mm, overlapping interval = 2.5 mm, and NEX = 0.74. Magnevist (Bayer Healthcare, Berlin, Germany) was injected into the cubital vein using a high-pressure injector (Spectris, Medrad, Pittsburgh, PA) at a dose of 0.2 mmol/kg and a flow rate of 3.0 mL/s. The contrast agent was rinsed using 15 mL of normal saline to ensure that it had completely entered the body. In the arterial phase, portal phase, and delayed phase, the scanning times were respectively 18 s, 55 s, and 2–5 min after injecting the contrast agent.

2.3. Categorization of imaging findings

MRI data for all patients were acquired from the picture archiving and communication systems of our institution and were further evaluated, in reference to with the relevant literature and LI-RADS.[8] Two abdominal radiologists with more than 10 years of experience in abdominal imaging diagnosis evaluated the images. They did not know the pathologic results for the group. The evaluation of unenhanced MRI images included assessments of lesion location (left and right liver), size, shape (roundish or irregular), internal intensity (homogeneous or heterogeneous), internal components (calcification, necrosis, cystic change, or bleeding), and boundaries (clear or ill defined). Other signs, including liver surface retraction, pseudocapsule, disproportionate biliary dilatation, and enlarged lymph nodes, were also evaluated. With MRI, homogeneous or heterogeneous lesion intensity was observed in the T2WI sequence. The target sign in the diffusion-weighted imaging (DWI) sequence was defined as hyperintensity in the periphery and hypointensity in the center, in reference to Park et al's[13] research. The apparent diffusion coefficient (ADC) value of tumor was also measured and expressed as the average of 3 measurements with appropriate region of interest. On contrast-enhanced MRI, lesion enhancement in the arterial phase, portal phase, and delayed phase were evaluated. The lesion enhancement degree included globally hyperintense, partially hyperintense, peripherally hyperintense, isointense, and hypointense. Lesion enhancement patterns were also evaluated and included peripheral enhancement, progressive enhancement, peripheral continuous enhancement, stable hyperenhancement, stable hypoenhancement, and wash-in with wash-out enhancement. Progressive enhancement was defined as a continuous range of lesion enhancement over time but not including peripheral continuous enhancement. Stable hyperenhancement was defined as a lesion that was hyperintense relative to the peripheral hepatic tissue in each phase of the enhanced scan, and the scope of lesion enhancement did not expand over time. Stable hypoenhancement was defined as a lesion that was hypointense relative to the peripheral hepatic tissue in each phase of the enhanced scan.

2.4. Statistical analysis

Quantitative variables, including patient age; lesion size; liver function indices, including serum alanine aminotransferase (ALT), aspartic transaminase (AST), total bilirubin (TBIL),

direct bilirubin (DBIL), and indirect bilirubin (IBIL); and tumor markers, including serum α-fetoprotein (AFP), carcinoembryonic antigen (CEA), carbohydrate antigen 199 (CA 199), and carbohydrate antigen 125 (CA 125), are expressed as medians and ranges. Categorical variables, including clinical symptoms, signs, clinical histories, abnormal liver function, and abnormal tumor markers, are expressed as counts and proportions. The SPSS software package, version 19.0, was used for statistical analysis, and data enumeration was performed using the χ^2 test for analysis, including comparisons of ICC enhancement degrees and patterns between different diameter groups on contrast-enhanced MRI. $P < .05$ indicated a significant difference between the groups.

3. Results

3.1. Clinical data

In total, 41 patients with small ICC with certain pathological diagnoses, all with single nodules, were included there were 40 cases of surgical excision and 1 case of ultrasound biopsy. There were 31 men and 11 women, for a ratio of approximately 3:1. The age of onset ranged from 38 to 71 years, and the average age was 56.33 ± 8.55 years. Intrahepatic lesions were found in 31 patients without clinical symptoms by physical examinations or clinical screenings; 12 patients had clinical symptoms. The abnormal liver function indices identified by laboratory testing included the following: 5 patients with elevated ALT [range, 48–79 U/L; average, 67.60 ± 15.40 U/L (reference range, 5–40 U/L)], 4 patients with elevated AST [range, 54–74 U/L; average, 61.50 ± 8.81 U/L (reference range, 8–40 U/L)], 11 patients with elevated TBIL [range, 15–34 μmol/L; average, 25.82 ± 5.95 μmol/L (reference range, 0–21 μmol/L)], 11 patients with elevated DBIL [range, 6–19 μmol/L; average, 8.64 ± 3.59 μmol/L (reference range, 0–5 μmol/L)], and 6 patients with elevated IBIL [range, 16–25 μmol/L; average, 18.50 ± 3.27 μmol/L (reference range, 3–14 μmol/L)]. Forty patients underwent tumor marker detection, and elevations in the following tumor markers were identified: 1 patient with elevated AFP [779 ng/mL (reference range, 0–20 ng/mL)], 5 patients with elevated CEA [range, 5–18 ng/mL; average, 9.12 ± 5.21 ng/mL (reference range, 0–5 ng/mL)], 9 patients with elevated CA 199 [range, 43–7364 U/mL; average, 1342.65 ± 2836.43 U/mL (reference range, 0–37 U/mL)], and 3 patients with elevated CA 125 [range, 35–83 U/mL; average, 56.43 ± 20.31 U/mL (reference range, 0–35 U/mL)]. The clinical data are summarized in Table 1.

Table 1

Demography of patients with small intrahepatic cholangiocarcinoma.

Item	Quantization
Patients, No.	41
Sex	
Male, No. (%)	30 (73)
Female, No. (%)	11 (27)
Age, mean year (range)	56
Asymptomatic (%)	31 (76)
Abdominal pain (%)	5 (12)
Abdominal distension (%)	2 (5)
Stomach problems (%)	2 (5)
Abdominal mass (%)	1 (2)
Weight loss (%)	2 (5)
Hepatitis B virus (%)	25 (61)
Fatty liver (%)	5 (12)
Cholelithiasis (%)	8 (20)
Schistosome hepatic disease (%)	1 (2)
Diabetes (%)	2 (5)
Hypertension (%)	6 (15)
Other cancer histories (%)	4 (10)
Drinking (%)	12 (29)
Smoking (%)	18 (44)
Alanine aminotransferase (%)	5 (12)
Aspartic transaminase (%)	4 (10)
Total bilirubin (%)	11 (27)
Direct bilirubin (%)	11 (27)
Indirect bilirubin (%)	6 (15).
α-Fetoprotein* (%)	1 (3)
Carcinoembryonic antigen* (%)	5 (13)
Carbohydrate antigen 199* (%)	9 (23)
Carbohydrate antigen 125* (%)	3 (8)

* Forty patients underwent tumor marker detection.

3.2. Magnetic resonance imaging findings

3.2.1. Small intrahepatic cholangiocarcinoma imaging features on unenhanced magnetic resonance imaging. Forty-one patients with small ICC underwent unenhanced MRI, and 40 of them underwent DWI sequence detection. Lesions were located in the right liver in 21 patients and in the left liver in 20 patients. The average lesion size was 2.26 ± 0.50 cm. Thirty-two patients had roundish lesions, and 9 patients had irregular lesions. On T1WI, the lesions showed hypointensity, while they showed hyperintensity on T2WI imaging. Sixteen patients had homogeneous lesions, and 25 patients had heterogeneous lesions. One patient had calcification, 2 patients had necrosis, and 4 patients had cystic changes. Thirty-five patients had a lesion with a clear boundary, and 6 patients had a lesion with an ill-defined boundary. In addition, 2 patients had liver surface retraction, 4 patients had disproportionate biliary dilatation, and 4 patients had enlarged lymph nodes. On contrast-enhanced MRI examination, there were 2 patients with pseudocapsule. In the DWI sequence, 17 patients had mild hyperintensity and 23 patients had moderate or significant hyperintensity. The average ADC value of tumors was $1.28 \pm 0.40 \times 10^{-3}$ mm^2/s. The target sign was observed in 14 patients on DWI. No internal hemorrhage was seen on the MRI scans.

3.2.2. Imaging features of small intrahepatic cholangiocarcinoma on contrast-enhanced magnetic resonance imaging. Forty-one patients with small ICC underwent contrast-enhanced MRI examination. In the arterial phase, 10 patients had globally hyperintense lesions, 11 patients had partially hyperintense lesions, 16 patients had peripherally hyperintense lesions, and 4 patients had hypointense lesions. In the portal phase, 9 patients had globally hyperintense lesions, 11 patients had partially hyperintense lesions, 6 patients had peripherally hyperintense lesions, 2 patients had isointense lesions, and 13 patients had hypointense lesions. In the delayed phase, 11 patients had globally hyperintense lesions, 10 patients had partially hyperintense lesions, 2 patients had peripherally hyperintense lesions, 6 patients had isointense lesions, and 12 patients had hypointense lesions. The enhancement patterns for small intrahepatic cholangiocarcinoma included peripheral enhancement in 2 patients, peripheral continuous enhancement in 15 patients (Fig. 1), progressive enhancement in 10 patients (Figs. 2 and 3), stable hyperenhancement in 7 patients (Fig. 4), stable hypoenhancement in 1 patient, and wash-in with wash-out enhancement in 6 patients.

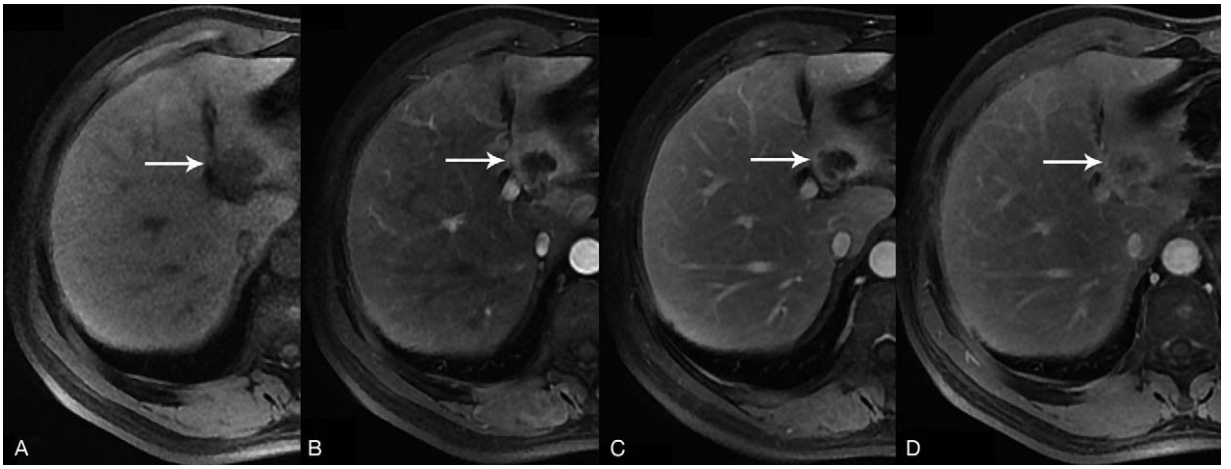

Figure 1. Magnetic resonance imaging (MRI) scan of a 46-year-old male patient with a 2.6-cm-diameter ICC nodule in the left hepatic lobe (A, arrows). The lesion shows peripheral hyperintensity in the arterial phase (B) and its hyperintensity increases over time in the portal phase (C) and delayed phase (D).

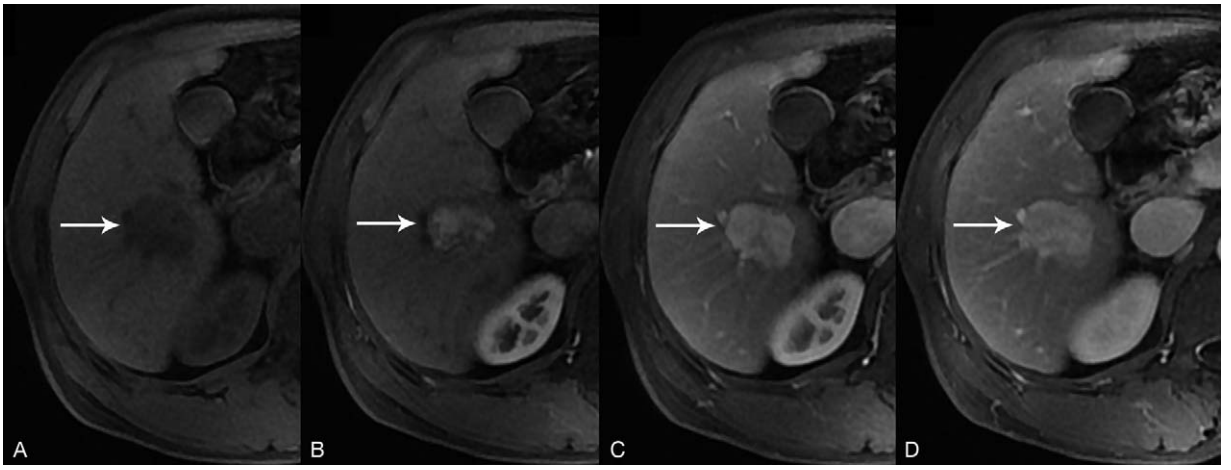

Figure 2. Magnetic resonance imaging (MRI) scan of a 57-year-old male patient with a 2.9-cm-diameter ICC nodule in the right hepatic lobe (A, arrows). The lesion shows partly hyperintensity in the arterial phase (B) and its hyperintensity increases over time in the portal phase (C) and delayed phase (D).

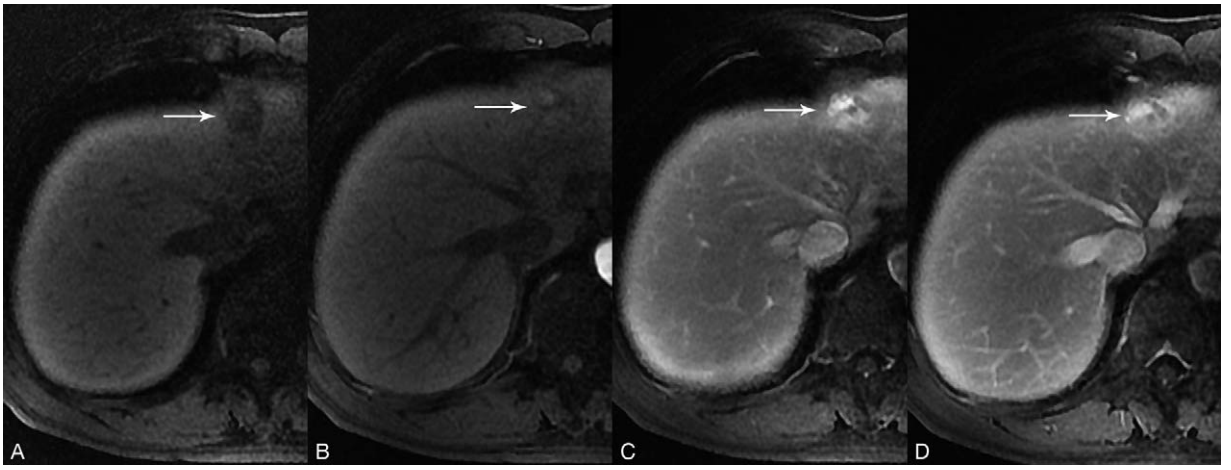

Figure 3. Magnetic resonance imaging (MRI) scan of a 50-year-old male patient with a 1.7-cm-diameter ICC nodule in the left hepatic lobe (A, arrows). The lesion shows partly hyperintensity enhancement in the arterial phase (B), and its hyperintensity increases over time in the portal phase (C) and delayed phase (D).

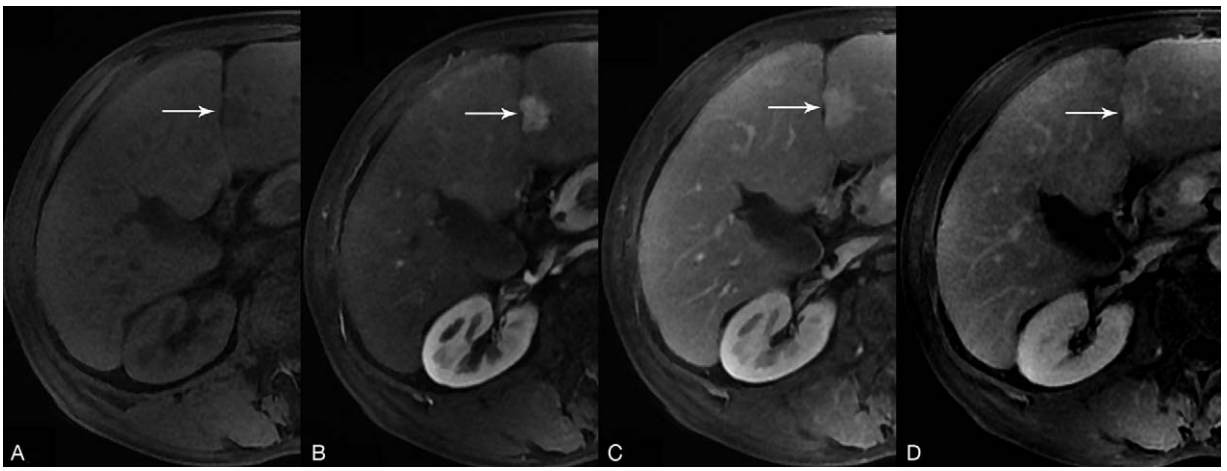

Figure 4. Magnetic resonance imaging (MRI) scan of a 51-year-old male patient with a 1.9-cm-diameter ICC nodule in the left hepatic lobe (A, arrows). The lesion shows global enhancement in the arterial phase (B), and its hyperintensity persistent over time in the portal phase (C) and delayed phase (D).

3.2.3. Contrast-enhanced magnetic resonance imaging features of small intrahepatic cholangiocarcinoma in different diameter groups. Sixteen patients had ICC nodules with a diameter $\leq$2 cm. Twenty-five patients had ICC nodules with a diameter $>$2 cm and $\leq$3 cm. The lesion enhancement degrees and patterns on enhanced MRI are summarized in Tables 2 and 3, respectively.

3.2.4. Comparison of contrast-enhanced magnetic resonance imaging features of small intrahepatic cholangiocarcinoma in different diameter groups. In the arterial phase, smaller diameter nodules were most commonly globally hyperintense (38%), followed by partially hyperintense (25%) and hypointense (25%). In contrast, larger diameter nodules were most commonly peripherally hyperintense, followed by partially hyperintense. Statistical differences were found in the peripheral hyperintensity and hypointensity of small ICC nodules with different diameters in the arterial phase on contrast-enhanced MRI (P=.005 and P=.036). Twelve percent of the lesions with smaller diameters showed peripheral hyperintensity in the arterial phase, whereas 56% of lesions with larger diameters showed peripheral hyperintensity. In the arterial phase, 25% of lesions in the smaller diameter group showed hypointensity, while there was no hypointensity in the larger diameter group. There were no statistical differences in the appearance of other phases of contrast-enhanced MRI between the 2 groups. The comparison of the contrast-enhanced MRI appearances of the 2 groups is summarized in Table 2.

Nodules with a smaller diameter most commonly showed progressive enhancement (38%), followed by stable hyperenhancement (19%) and wash-in with wash-out enhancement (19%). In contrast, nodules with a larger diameter most commonly showed peripheral continuous enhancement (56%), followed by progressive enhancement (16%) and stable hyperenhancement (16%). Statistical differences were observed in peripheral enhancement patterns on contrast-enhanced MRI between lesions with different diameters (P=.001). There were no statistical differences in the other enhancement patterns. The comparison of enhancement patterns on contrast-enhanced MRI between the 2 groups is summarized in Table 3.

Table 2

Enhancement degree and comparison of 2 groups of small intrahepatic cholangiocarcinoma with diameters $\leq$2 cm (n = 16) and $>$2 cm (n = 25) on contrast-enhanced magnetic resonance imaging.

	Globally hyperintense	Partially hyperintense	Peripherally hyperintense	Isointense	Hypointense
Arterial phase					
Smaller nodule (%)	6 (38)	4 (25)	2 (12)	0 (0)	4 (25)
Larger nodule (%)	4 (16)	7 (28)	14 (56)	0 (0)	0 (0)
χ^2	1.419	0.022	7.758	–	4.377
P	*.234*	*.881*	***.005****	–	***.036****
Portal phase					
Smaller nodule (%)	4 (25)	3 (19)	2 (13)	2 (12)	5 (31)
Larger nodule (%)	5 (20)	8 (32)	4 (16)	0 (0)	8 (32)
χ^2	0	0.328	0.021	1.144	0.003
P	*.992*	*.567*	*.886*	*.285*	*.960*
Delayed phase					
Smaller nodule (%)	5 (31)	2 (13)	0 (0)	2 (12)	7 (44)
Larger nodule (%)	6 (24)	8 (32)	2 (8)	4 (16)	5 (20)
χ^2	0.022	1.093	0.174	0.021	1.635
P	*.881*	*.296*	*.677*	*.886*	*.201*

* $P<.05$, significant difference between both groups.

Table 3

Enhancement pattern and comparison of 2 groups of small intrahepatic cholangiocarcinoma with diameters ≤ 2 cm and >2 cm on contrast-enhanced magnetic resonance imaging.

	Contrast-enhanced MRI			
	Smaller nodule	Larger nodule	χ^2	*P*
Peripheral enhancement (%)	2 (12%)	0 (0%)	1.144	*.285*
Progressive enhancement (%)	6 (38%)	4 (16%)	1.419	*.234*
Peripheral continuous enhancement (%)	1 (6%)	14 (56%)	10.408	***.001****
Persistent hyperenhancement (%)	3 (19%)	4 (16%)	0.039	*.844*
Persistent hypoenhancement (%)	1 (6%)	0 (0%)	0.052	*.820*
Washout enhancement (%)	3 (19%)	3 (12%)	0.021	*.886*

* $P < .05$, significant difference between both groups.
MRI = magnetic resonance imaging.

4. Discussion

In this study, most cases of small ICC (32/41) were found during physical examinations or clinical screenings and lacked clinical symptoms. Only a small proportion of patients with small ICC had specific symptoms, such as abdominal pain, abdominal distension, and weight loss, consistent with a previous description of ICC.[7] In the present research, more than half of the patients had a history of hepatitis B, some patients had cholelithiasis or fatty liver, and a certain proportion of patients had bad lifestyle habits, including smoking and alcohol abuse. These behaviors are considered risk factors for ICC.[7] Tumour markers for ICC, including Ca 199 and CEA, were detected in the present study. It was reported that the sensitivity and specificity of Ca 199 as a tumor marker for ICC are 62% and 63%, respectively.[7] In patients with ICC associated with primary sclerosing cholangitis, using a Ca 199 cut-off of 129 U/mL increased the sensitivity and specificity to 79% and 98%, respectively.[1] In contrast, in the present study, only approximately 24% (10/42) of the patients with ICC showed increased serum Ca 199 levels, perhaps because of the different risk factors for ICC. In the West, primary sclerosing cholangitis is an important risk factor for ICC and is often accompanied by an increase in Ca 199.[1] Therefore, imaging screenings are needed for people at high risk for ICC.

The unenhanced MRI imaging findings associated with small ICC in our study were similar to those of small HCC, which often lacks the typical large ICC characteristics of liver surface retraction and disproportionate biliary dilatation. The unenhanced MRI findings in our study are in accordance with the conclusions of previous studies.[13–15] However, it was reported that a target sign in a DWI sequence occurred in approximately 75% (24/32) of cases of small ICC, and DWI is believed capable of distinguishing ICC from HCC.[13] However, in our study, only approximately one third of the cases had the target sign. Furthermore, approximately 10% (4/41) of the patients had a history of other cancers, which reduced the diagnostic value of the target sign because it was necessary to consider the possibility of a metastatic tumor. Recent research also confirms that the diffusion restriction degree of ICC in the DWI sequence may be a prognostic marker.[16] In our study, the ADC value of small ICC is closer to group 2,[16] and its prognosis is better. Based on our clinical experience, our study confirmed the diffusion restriction degree of ICC is correlated with the tumor sizes.

In the arterial phase of contrast-enhanced MRI, small ICC was characterized by peripheral hyperdensity or hyperintensity, and the enhancement pattern was mainly peripheral enhancement and/or progressive enhancement, consistent with the results of Sheng's study of ICC.[14] However, slightly larger ICC nodules showed peripheral continuous enhancement, similar to another previous study,[17] whereas smaller nodules showed progressive enhancement. Surprisingly, 15% of our cohort showed a wash-in with wash-out enhancement pattern on contrast-enhanced MRI. Although there was no typical HCC enhancement pattern on contrast-enhanced CT in Iavarone et al's study,[10] 6.3% of cases in Sheng et al's[14] study had a wash-out enhancement pattern on contrast-enhanced MRI. In an earlier study, the wash-out enhancement pattern was even more common (5/8 patients) in small ICC on contrast-enhanced CT.[11] As understanding of the wash-in with wash-out imaging characteristic increases,[18] the differences between our results and those from other studies may be explained. A recent study indicated that 15% of ICC nodules show a wash-in with wash-out enhancement pattern on MRI.[19] We believe that this type of enhancement, which is similar to HCC, requires continuous attention, especially for patients with liver cirrhosis. However, there was no correlation between the proportion of lesions with a wash-in with wash-out enhancement pattern and the diameters of these lesions. Furthermore, we agree that determining whether these nodules have pseudocapsules might be a valuable identification sign.[13]

On contrast-enhanced MRI, small ICC can be characterized by global hyperintensity in each phase, and 17% of nodules showed stable hyperenhancement in this modality. Furthermore, it has been confirmed that stable enhancement is usually related to high-grade ICC.[20] Thus, small ICC nodules must be differentiated from common benign hypervascular lesions or other uncommon lesions, such as intrahepatic bile duct adenoma.[21] On contrast-enhanced MRI, smaller nodules showed more global hyperintensity in the arterial phase. Confirming this trend, we found that smaller nodules were characterized by a greater degree of arterial global enhancement, whereas larger nodules were characterized by a greater degree of peripheral enhancement in the arterial stage.[11] Furthermore, more than half of the larger nodules showed peripheral continuous enhancement, whereas the smaller nodules had more diverse enhancement patterns, and only approximately one third were characterized by progressive enhancement (the most common enhancement pattern). Smaller nodules usually lack fibrous scarring in the center, which is considered the basis of peripheral enhancement.[11] Therefore, we also needed to distinguish these nodules from hemangioma. Finally, hypointensity mainly occurred in the smaller nodule group in the arterial phase on contrast-enhanced MRI. Based on these results, we believe that false low uptake of contrast agent caused by the fixed scanning time in the arterial phase must be excluded. Another possible explanation for these findings is the presence of immature arterial vascularization.[11] In the future, the imaging features of ICC must be standardized to a greater

extent to increase the evidence base needed to resolve dilemmas in identifying small HCC and ICC faced by radiological specialists,[22] as well as to categorize differences in the arterial phase according to LI-RADS, Organ Procurement and Transplantation Network and American Association for the Study of Liver Diseases guidelines.[23]

This study had some weaknesses and limitations. First, only a small number of cases were assessed. Although ICC is the second most common liver parenchyma primary malignant tumor, it is not easy to detect because it often has no symptoms. Although our center is one of the largest in China for the diagnosis and treatment of liver cancer and despite the fact that China has such a large population, our cohort remained small. However, compared to other published reports of small ICC, our cohort size is acceptable. In the future, improved imaging screening and engagement in multicenter joint research are feasible methods to overcome the small number of patients with small ICC. Second, small ICC is relatively rare, resulting in long time spans between the included patients in this study. This affected the consistency of the research due to several uncontrollable factors, such as replacement of imaging examination equipment, updates in scanning sequences and parameter optimization, and upgrades in contrast material. Moreover, the images were independently evaluated by 2 experienced radiologists at our own institution, but we attempted to avoid relaying directional clinical information to ensure that reading of the radiographs was objective as possible. The radiologists referred to imaging feature definitions included in LI-RADS; however, this resource is more focused on HCC. As such, the classification and description of ICC enhancement were not sufficiently detailed. Therefore, as understanding of ICC, especially small ICC, increases, the classification of the disease and the definitions of its imaging features must be further updated.

In conclusion, different imaging findings for small-diameter mass-forming ICC were clearly observed between nodules with different diameters on contrast-enhanced MRI. Small ICC nodules commonly showed peripheral continuous enhancement; however, the smallest nodules studied commonly showed progressive enhancement. In addition, a subset of small ICC nodules showed stable hyperenhancement and wash-in with wash-out enhancement.

References

[1] Razumilava N, Gores GJ. Cholangiocarcinoma. Lancet 2014;383:2168–79.

[2] Rizvi S, Gores GJ. Pathogenesis, diagnosis, and management of cholangiocarcinoma. Gastroenterology 2013;145:1215–29.

[3] Tyson GL, El-Serag HB. Risk factors for cholangiocarcinoma. Hepatology 2011;54:173–84.

[4] Razumilava N, Gores GJ. Combination of gemcitabine and cisplatin for biliary tract cancer: a platform to build on. J Hepatol 2011;54:577–8.

[5] DeOliveira ML, Cunningham SC, Cameron JL, et al. Cholangiocarcinoma: thirty-one-year experience with 564 patients at a single institution. Ann Surg 2007;245:755–62.

[6] Everhart JE, Ruhl CE. Burden of digestive diseases in the United States Part III: liver, biliary tract, and pancreas. Gastroenterology 2009;136:1134–44.

[7] Bridgewater J, Galle PR, Khan SA, et al. Guidelines for the diagnosis and management of intrahepatic cholangiocarcinoma. J Hepatol 2014;60:1268–89.

[8] http://www.acr.org/Quality-Safety/Resources/LIRADS. Accessed October 1, 2017.

[9] Khan SA, Davidson BR, Goldin RD, et al. Guidelines for the diagnosis and treatment of cholangiocarcinoma: an update. Gut 2012;61:1657–69.

[10] Iavarone M, Piscaglia F, Vavassori S, et al. Contrast enhanced CT-scan to diagnose intrahepatic cholangiocarcinoma in patients with cirrhosis. J Hepatol 2013;58:1188–93.

[11] Kim SJ, Lee JM, Han JK, et al. Peripheral mass-forming cholangiocarcinoma in cirrhotic liver. AJR Am J Roentgenol 2007;189:1428–34.

[12] Rimola J, Forner A, Reig M, et al. Cholangiocarcinoma in cirrhosis: absence of contrast washout in delayed phases by magnetic resonance imaging avoids misdiagnosis of hepatocellular carcinoma. Hepatology 2009;50:791–8.

[13] Park HJ, Kim YK, Park MJ, et al. Small intrahepatic mass-forming cholangiocarcinoma: target sign on diffusion-weighted imaging for differentiation from hepatocellular carcinoma. Abdom Imaging 2013;38:793–801.

[14] Sheng RF, Zeng MS, Rao SX, et al. MRI of small intrahepatic mass-forming cholangiocarcinoma and atypical small hepatocellular carcinoma ($\leq$3 cm) with cirrhosis and chronic viral hepatitis: a comparative study. Clin Imaging 2014;38:265–72.

[15] Adam SZ, Parthasarathy S, Miller FH. Intrahepatic cholangiocarcinomas mimicking other lesions. Abdom Imaging 2015;40:2345–54.

[16] Lee J, Kim SH, Kang TW, et al. Mass-forming intrahepatic cholangiocarcinoma: diffusion-weighted imaging as a preoperative prognostic marker. Radiology 2016;281:119–28.

[17] Kang Y, Lee JM, Kim SH, et al. Intrahepatic mass-forming cholangiocarcinoma: enhancement patterns on gadoxetic acid-enhanced MR images. Radiology 2012;264:751–60.

[18] Kim R, Lee JM, Shin CI, et al. Differentiation of intrahepatic mass-forming cholangiocarcinoma from hepatocellular carcinoma on gadoxetic acid-enhanced liver MR imaging. Eur Radiol 2016;26:1808–17.

[19] Li R, Cai P, Ma KS, et al. Dynamic enhancement patterns of intrahepatic cholangiocarcinoma in cirrhosis on contrast-enhanced computed tomography: risk of misdiagnosis as hepatocellular carcinoma. Sci Rep 2016;26:26772.

[20] Ciresa M, De Gaetano AM, Pompili M, et al. Enhancement patterns of intrahepatic mass-forming cholangiocarcinoma at multiphasic computed tomography and magnetic resonance imaging and correlation with clinicopathologic features. Eur Rev Med Pharmacol Sci 2015;19:2786–97.

[21] Liang W, Xu S. Magnetic resonance imaging findings of intrahepatic bile duct adenoma: a report of 4 cases. J Comput Assist Tomogr 2015;39:747–51.

[22] Merkle EM, Zech CJ, Bartolozzi C, et al. Consensus report from the 7th International Forum for Liver Magnetic Resonance Imaging. Eur Radiol 2016;26:674–82.

[23] Mitchell DG, Bruix J, Sherman M, et al. LI-RADS (Liver Imaging Reporting and Data System): summary, discussion, and consensus of the LI-RADS Management Working Group and future directions. Hepatology 2015;61:1056–65.